

THE FORMATION EPOCH OF EARLY-TYPE GALAXIES IN THE $Z \sim 0.9$ CL1604 SUPERCLUSTER

N. L. HOMEIER¹, S. MEI¹, J.P. BLAKESLEE², M. POSTMAN³, B. HOLDEN⁴, H. C. FORD¹, L. D. BRADLEY¹, R. DEMARCO¹,
M. FRANX⁶, G. D. ILLINGWORTH⁴, M.J. JEE¹, F. MENANTEAU¹, P. ROSATI⁵, A. VAN DER WEL¹, A. ZIRM¹

Draft version September 23, 2018

ABSTRACT

We analyse the cluster color-magnitude relation (CMR) for early-type galaxies in two of the richer clusters in the $z \sim 0.9$ supercluster system to derive average ages and formation redshifts for the early-type galaxy population. Both clusters were observed with the Advanced Camera for Surveys aboard the *Hubble Space Telescope* through the F606W and F814W filters, which brackets the rest-frame 4000 Å break at the cluster redshifts of $z \sim 0.9$. We fit the zeropoint and slope of the red cluster sequence, and model the scatter about this relation to estimate average galaxy ages and formation redshifts. We find intrinsic scatters of 0.038–0.053 mag in ($V_{606} - I_{814}$) for the E and E+S0 populations, corresponding to average ages of 3.5–3.7 Gyr and formation redshifts $z_f = 2.4 - 2.6$. We find at least one significant difference between the CL1604+4304 and 4321 early-type CMRs. 4321, the less X-ray luminous and massive of the two, lacks bright L^* ellipticals. We combine the galaxy samples to fit a composite CMR down to 0.15 L^* , and find that the slope of the combined cluster CMR is significantly steeper than for RX J0152.7-1357 but consistent with MS 1054-03, both at similar redshift. The slope of the CL1604 CMR at the bright end ($L > 0.5 L^*$) is flatter and consistent with the CMR slopes found for other high redshift clusters. We find evidence for increasing scatter with increasing magnitude along the early-type CMR, consistent with a 'downsizing' scenario, indicating younger mean ages with decreasing galaxy mass.

Subject headings: galaxies: clusters: individual (CL1604) - galaxies: elliptical and lenticular - galaxies: evolution

1. INTRODUCTION

The majority of elliptical galaxies appear to have formed the bulk of their stars at very early times. In the local universe, elliptical galaxies over a wide range of environment follow a tight color-magnitude relation (CMR) with extremely small scatter (Visvanathan & Sandage 1977; Bower et al. 1992; Hogg et al. 2004; McIntosh et al. 2005). In a galaxy cluster, there is an obvious bimodality in galaxy colors that is well-correlated with galaxy morphology. The 'blue cloud' is dominated by spiral and irregular galaxies, and the prominent ridge of red galaxies is composed mainly of ellipticals and S0s. More massive red sequence galaxies are on average older, more metal-rich, and contain relatively more products of core-collapse supernovae, indicating more rapid formation, than lower mass red sequence galaxies (Bernardi et al. 2005; Nelan et al. 2005).

The early-type cluster CMR, or red cluster sequence, is such a regular feature that it can be used to find rich galaxy clusters at $z > 1$ (e.g. Gladders & Yee 2005). The origin of the slope of the CMR is generally accepted as a mass-metallicity relation, where more massive galaxies have higher metallicities (e.g. Kodama & Arimoto 1997). The scatter about the CMR is related to age

differences at a given galaxy mass. The tightness of the CMR and its lack of observed evolution with redshift implies that CMR galaxies formed at high redshift, $z > 2$. Since galaxies change color more quickly at younger ages, pushing CMR observations to higher redshifts allows us to more accurately determine the formation redshifts of early-type galaxies.

The ACS Intermediate Redshift Cluster Survey (Ford et al. 2004) covers 8 clusters in the redshift range $0.8 < z < 1.3$ with the Advanced Camera for Surveys (ACS; Ford et al. 1998) aboard the *Hubble Space Telescope* as part of the ACS Guaranteed Time Observations (GTO) program. Of the previous results, the most relevant to the current study are the analyses of the CMR in the $z = 1.24$ cluster RDCS J1252.9-2927 (Blakeslee et al. 2003b), the $z = 1.1$ cluster RDCS J0910+5422 (Mei et al. 2006a), two clusters in the $z = 1.27$ Lynx supercluster CL0848 (Mei et al. 2006b), and two $z \sim 0.83$ clusters, MS 1054-03 and RX J0152.7-1357 (Blakeslee et al. 2006). These four studies spanning 6 clusters found small intrinsic scatters of 0.03–0.06 mag about the CMR, average luminosity-weighted ages of 2.2–3.5 Gyr, and formation redshifts of $z > 2.3 - 2.7$ in a concordance Λ CDM cosmology.

In this paper we extend these early-type CMR studies to include two clusters at the low-mass end of previously studied clusters. We present an analysis of two low X-ray luminosity clusters in the CL1604 supercluster, CL1604+4304 and 4321, which have been previously studied in some detail (Gunn et al. 1986; Castander et al. 1994; Oke et al. 1998; Postman et al. 1998; Stanford et al. 1998; Lubin et al. 2000; Postman et al. 2001; Stanford et al. 2002; Holden et al. 2004). Wide field imaging of

¹ Department of Physics and Astronomy, Johns Hopkins University, 3400 North Charles Street, Baltimore, MD 21218.

² Department of Physics and Astronomy, Washington State University, Pullman, WA, 99164-2814.

³ STScI, 3700 San Martin Drive, Baltimore, MD 21218.

⁴ UCO/Lick Observatory, University of California, Santa Cruz, CA 95064.

⁵ European Southern Observatory, Karl-Schwarzschild-Strasse 2, D-85748 Garching, Germany.

⁶ Leiden Observatory, Postbus 9513, 2300 RA Leiden, Netherlands.

the surrounding regions uncovered red galaxies with colors consistent with passive galaxies at $z \sim 0.9$ (Lubin et al. 2000), and follow-up spectroscopy confirmed the existence of a supercluster (Gal & Lubin 2004). Cl1604+4304 has a velocity dispersion of $962 \pm 141 \text{ km s}^{-1}$ from 67 redshifts (Gal & Lubin 2004), and a relatively low temperature and luminosity: $T_X = 2.51_{-0.69}^{+1.05} \text{ keV}$ and $L_{X,bol} = 2.0 \times 10^{44} \text{ ergs s}^{-1}$ (Lubin et al. 2004). Cl1604+4321 has a velocity dispersion of $640 \pm 71 \text{ km s}^{-1}$ (Gal & Lubin 2004). Cl1604+4321 was not detected by *ROSAT*, and has an upper limit on the 0.1 – 2.4 keV X-ray luminosity of $L_x \leq 4.76 \times 10^{43} \text{ erg s}^{-1}$, compared to the 0.1 – 2.4 keV detection of Cl1604+4304 of $L_x = 7.43 \pm 1.59 \times 10^{43} \text{ erg s}^{-1}$ (Postman et al. 2001). Based on their measured velocity dispersions, Cl1604+4321 is at least a factor of ~ 2 less massive than Cl1604+4304.

The paper is organized as follows. In § 2 we describe the observations, object selection, and photometry. In § 3 we present our color-magnitude diagrams. § 4 discusses the results of the CMR fits, § 5 and 6 discuss the CMR scatter as a function of magnitude and comparisons to other work, and in § 7 we present our conclusions.

2. OBSERVATIONS AND REDUCTIONS

CL1604+4304 and CL1604+4321 were observed with the ACS Wide Field Channel as part of a guaranteed time observation program (proposal 9290). These clusters were observed for 2 orbits in each V_{606} and I_{814} at a single pointing. The data were processed with the *Apsis* pipeline (Blakeslee et al. 2003a). Our photometry is calibrated to the AB magnitude system using zeropoints from Sirianni et al. (2005). Object detection and photometry was performed by SExtractor (Bertin & Arnouts 1996) incorporated within the *Apsis* pipeline. A more detailed description can be found in Benítez et al. (2004). We use MAG_AUTO when quoting total broad-band magnitudes, as this is the best estimate of a galaxy’s total magnitude (Benítez et al. 2004). Zeropoints for the V_{606} and I_{814} filters are 26.486 and 25.937 AB magnitudes, respectively. We correct the galaxy magnitudes and colors for Galactic extinction: this amounts to 0.033 ± 0.005 in V_{606} and 0.021 ± 0.003 in I_{814} for CL1604+4304, 0.039 ± 0.006 in V_{606} and 0.024 ± 0.004 in I_{814} for CL1604+4321.

Extensive visual morphology catalogs were created by MP (Postman et al. 2005). Morphologies were determined visually on the T-type system (de Vaucouleurs et al. 1991). All galaxies in the field with $I_{814} \leq 24$ magnitude were classified. Approximately 10% of the galaxies were also classified by three independent classifiers to estimate the classification errors. Majority agreement was achieved for 75% of objects with $i_{775} \leq 23.5$. There was no significant systematic offset between the mean classification from the independent classifiers. More information can be found in Postman et al. (2005). A T-type $-5 \leq T \leq -3$ corresponds to elliptical galaxies, $-2 \leq T \leq -1$ corresponds to lenticular (S0) galaxies, $T=0$ to S0/a galaxies, and $T > 0$ to Sa and later-type galaxies.

We adopt $M_B^* = -21.3$ AB mag from the Schechter function fit to galaxies in the 2dF survey (Norberg et al. 2002) and -1.04 magnitudes of luminosity evolution at

$z = 0.90$ (van Dokkum & Stanford 2003; Holden et al. 2005). This corresponds to an observed magnitude of $I_{814}^* = 21.9$ at $z = 0.90$ for an early-type spectrum with $V_{606} - I_{814} = 1.8$, using the conversion $I_{814} = M_B + 43.820 + 0.089 \times (V_{606} - I_{814}) - 0.794$ obtained from the BC03 solar metallicity single burst models with a Salpeter IMF. Thus, our visual morphological classification extends to $0.15 L^*$. Throughout this paper we use $H_0 = 70 \text{ km s}^{-1} \text{ Mpc}^{-1}$, $\Omega_m = 0.30$, and $\Omega_\Lambda = 0.70$.

We select all galaxies with $T \leq 0$ brighter than $I_{814} = 24.0$ mag. Because early-type galaxies have color gradients that can bias the measurement of the CMR, we measure galaxy colors within fixed spatial apertures defined in the reddest filter. We produce 80×80 pixel cutouts and subtract the background image produced by SExtractor. Other objects in the cutout are masked, and we fit a single psf-convolved Sersic profile with GALFIT (Peng et al. 2002), with the position, orientation, ellipticity, and effective radius as free parameters. The n index was constrained to be between $0.1 \leq n \leq 4$, and the ‘sky’ was fixed at 0. We ‘clean’ the cutouts with the CLEAN algorithm to remove the blurring of the PSF (Högbom 1974; Blakeslee et al. 2003b). The residuals are added back to the ‘cleaned’ images to conserve flux, and photometry is performed within a circular aperture of $r_h = R_e \sqrt{b/a}$, derived from fitting the F814W image. If the derived r_h is less than 3 pixels, we set it to 3 pixels. Color errors are derived from the RMS images generated in the *Apsis* pipeline (Blakeslee et al. 2003a). These images have estimated errors per pixel, including Poisson flux errors, read noise, cosmic ray rejection, dark, and bias frame errors. The RMS errors should be close to but slightly smaller than the true errors, due to correlated errors as a result of the geometric correction.

3. THE COLOR MAGNITUDE RELATION

We fit linear relations of the form:

$$(V_{606} - I_{814}) = slope(I_{814} - 23.) + c_0$$

where c_0 is the zeropoint and *slope* is the slope. For each cluster we fit the full early-type sample (E, S0, and Sa), as well as the Es, the S0s, and the Es+S0s. For Cl1604+4304 and the combined cluster sample, the fits were restricted to galaxies with colors $1.5 \leq V_{606} - I_{814} \leq 2.0$, then used an iterative linear fit with 2.5σ clipping based on Bisquare weighting (Press et al. 1992) and estimated the scatter with a biweight scale estimator (Beers et al. 1990). We note that linear least-squares fitting with 2.5σ clipping produced similar results. The 4321 CMR was less straightforward to fit than the Cl1604+4304 CMR. Restricting the initial sample to $1.5 \leq V_{606} - I_{814} \leq 2.0$, $1.6 \leq V_{606} - I_{814} \leq 2.0$, or within 0.06×3.0 mag of the Cl1604+4304 CMR all lead to different CMR slopes and scatters. The incompleteness of our spectroscopic sample for this field hampers our ability to accurately measure the 4321 CMR. In the end we chose to perform an initial clip around the Cl1604+4304 CMR, then used an iterative linear fit with 2.4σ clipping based on Bisquare weighting. However we discuss CMR results obtained from other initial clipping choices.

Uncertainties in the slopes, zeropoints, and scatters were derived with 10,000 bootstrap simulations. To estimate the intrinsic scatter about the fitted CMR we subtracted, in quadrature, the average galaxy color error

from the measured scatter. We also determined the mean scatter required to make the reduced χ^2 of the linear fit equal to 1. This method yielded intrinsic scatters lower by $\approx 10 - 20\%$, and are the values we quote.

The scatter about the CMR can be used to constrain the formation epoch of the CMR galaxies. Using a simple model that assumes that the difference in age is relatively constant as a function of magnitude (galaxy mass), the intrinsic scatter can be modeled in three ways. Following the method first used by van Dokkum et al. (2000), the first method assumes galaxies form in single bursts at random times between $t_0(z=5)$ and t_{end} . As we increase t_{end} , the mean age of the 10000 model galaxies increases, and the distribution of galaxy ages also narrows. We assume a minimum t_{end} of 0.5 Gyr. Galaxies need at least 0.5 Gyr after ceasing star formation to redden and arrive on the red cluster sequence. These models assume no correlation in galaxy formation times within a cluster halo. The relationship between intrinsic scatter, luminosity-weighted mean galaxy age, and t_{end} is shown in Fig. 2 for models with a Salpeter IMF and three metallicities ($Z=0.008, 0.02, 0.05$; Bruzual & Charlot (2003)). Another method assumes galaxies form stars at constant rates from random times t_1 and t_2 between t_0 and t_{end} . Again we vary t_{end} from 0.5 Gyr from the time of observation to t_0 . A third method is to assume exponentially declining star formation rates, starting and ending at random times t_1 and t_2 between t_0 and t_{end} . Previous studies have found that the ages derived from this constant star formation model are systematically lower by 10 – 20% (Blakeslee et al. 2003b). This is approximately what we find here for intrinsic scatters of 0.05 – 0.03 mag. However the largest changes in mean ages would be from metallicities lower than solar, according to the Bruzual & Charlot 2003 models. As is known from high-resolution spectroscopy in the local universe, massive elliptical galaxies have solar or super-solar metallicities, although it is not clear how smoothly the metallicity varies with luminosity along the red sequence. These models would predict a decreasing scatter with luminosity if the mean ages did not depend on luminosity.

In the following sections we quote constraints on galaxy ages and formation times from only the single burst method with solar metallicity. Errors on the ages and formation redshifts come from adding and subtracting the bootstrapped 1σ errors to the intrinsic scatter to derive the asymmetric 1σ limits on the average ages and formation redshifts.

We compare our fitted CMR relations to the relation for Coma from Bower et al. (1992). We transformed the $U - V$ slope and zeropoint to $U - B$ using the BC03 solar and super-solar 12-13 Gyr SSP models. From this we derived the relation: $\delta(U - B) = 0.66\Delta(U - V)$. Using the empirical Kinney-Calzetti elliptical, S0, and Sa templates (Kinney et al. 1996) and the Coleman elliptical template (Coleman et al. 1980) gave a similar result. We transformed the $U - B$ slope, -0.054 , to the $V_{606} - I_{814}$ slope of -0.066 at $z = 0.90$ with the derived relation $\delta(V_{606} - I_{814}) = 1.23\delta(U - B)$. This transformation depends somewhat on the templates used to derive the colors. With the empirical templates we derived the relations $\delta(U - B) = 0.51\Delta(U - V)$ and $\Delta(V_{606} - I_{814}) = 1.45\delta(U - B)$.

We convert the observed $V_{606} - I_{814}$ colors measured in AB magnitudes to rest-frame U-B measured in Vega magnitudes using the IRAF SYNPHOT package and the BC2003 $Z=0.008, 0.02, 0.05$ metallicity models with single bursts and ages between 1 – 6 Gyr. We performed a linear fit to these models and find $\delta(U - B) = 0.79\Delta(V_{606} - I_{814})$ at $z = 0.9$.

3.1. Redshift Color Corrections

The color difference in $V_{606} - I_{814}$ between a redshift of $z = 0.90$ and a redshift of $z = 0.92$ depends strongly on the underlying galaxy SED, if one considers the full range of galaxy types. For example, a galaxy matching a $z = 0$ S0 template spectrum would be 0.0041 mag redder at $z = 0.92$, while an Sa template spectrum would be 0.0130 mag redder, but an Sb template would be 0.006 mag bluer. The $V_{606} - I_{814}$ colors of the CMR galaxies fall between the Sa ($V_{606} - I_{814} = 1.82$ at $z = 0.90$) and Sb ($V_{606} - I_{814} = 1.51$ at $z = 0.90$) empirical templates, but the shape of the SED is not likely to match. Instead we use the Bruzual & Charlot (2003) single bursts and short exponentially declining SFR models and we find corrections of the order of $\Delta(V_{606} - I_{814}) = 0.02 - 0.8\Delta z$. The range in redshift for each cluster is $\Delta z \sim 0.01$, or maximum corrections of 0.008 in ($V_{606} - I_{814}$) color. These corrections are small enough that we neglect them.

3.2. CL1604+4304

The color-magnitude diagram of Cl1604+4304 is shown in Figure 3a. The red cluster sequence is prominent in the color-magnitude diagram of this cluster field. The fitting results are summarized in Table 1. For the E+S0 sample we find

$(V_{606} - I_{814}) = (-0.076 \pm 0.009) \times (I_{814} - 23) + 1.738 \pm 0.008$ and an intrinsic scatter of 0.038 ± 0.004 mag. The slopes, zeropoints, and scatters of the E+S0+Sa, E+S0, E, and S0 relations are consistent within the errors.

In Figure 4 we show the color magnitude diagram with elliptical galaxies as circles, S0s as squares, S0/a as stars, and late-type galaxies as triangles. Spectroscopically confirmed cluster members are indicated by open boxes. Two of the brightest four ellipticals are spectroscopically confirmed cluster members. Galaxies included in the CMR fit are indicated as larger filled symbols. The CMR relation is overplotted as a solid line, and the transformed Coma relation as a dashed line. Modeling the scatter about the red cluster sequence for the E+S0 sample with the stochastic single bursts, we find an average galaxy age of $3.71^{+0.04}_{-0.03}$ Gyr, with an average formation redshift $z_f = 2.60^{+0.03}_{-0.03}$. The Es and S0s do not have significantly different intrinsic CMR scatters, so we find similar ages and formation redshifts.

3.3. CL1604+4321

Visually, there are many more blue galaxies in the CL1604+4321 field than in the Cl1604+4304 field (see Fig. 3), the red cluster sequence appears less defined, and it lacks bright, $I_{814} < 21.5$ magnitude elliptical galaxies. The CMR fitting results are summarized in Table 2. Using an initial clip of 0.06×3 mag around the Cl1604+4304 CMR, we find for the E+S0 sample

$(V_{606} - I_{814}) = (-0.045 \pm 0.021) \times (I_{814} - 23) + 1.782 \pm 0.015$

and an intrinsic scatter of 0.053 ± 0.010 mag. For the E-only sample we find a slope of -0.066 ± 0.027 and an intrinsic scatter of 0.048 ± 0.011 mag. Again for this cluster, the slopes, zeropoints, and scatters of the E-only and S0-only relations are the same within 1σ errors.

For the E+S0 intrinsic scatter, with the single burst models we find an average age of $3.5_{-0.2}^{+0.2}$ Gyr, and $z_f = 2.44_{-0.12}^{+0.15}$. For the elliptical-only sample of 19 galaxies, we find an average age of $3.60_{-0.19}^{+0.12}$ Gyr, and a mean $z_f = 2.5_{-0.16}^{+0.1}$.

If we use the same color cuts and sigma-clipping when fitting the C11604+4304 and 4321 CMRs, the 4321 fitted CMR slopes are significantly flatter than the C11604+4304 CMR, and the intrinsic scatter is significantly larger than the C11604+4304 scatter. For example, using $1.5 \leq V_{606} - I_{814} \leq 2.0$ and 2.4σ clipping, the E+S0 sample the slope and intrinsic scatter are 0.00 ± 0.04 and 0.066 ± 0.009 . Shown in Fig. 5, this CMR includes elliptical galaxies redward of the Coma slope, and S0s with $V_{606} - I_{814} = 1.5 - 1.6$. Some or all of these galaxies may be interlopers. On the other hand, they may be cluster members which have yet to evolve to a tight CMR, and we are biasing the CMR slope and underestimating the intrinsic scatter with our initial cut about the C11604+4304 CMR. The E-only CMR slope and intrinsic scatter are -0.022 ± 0.037 and 0.062 ± 0.011 , still significantly flatter and with more scatter than the E-only slope initially clipped around the C11604+4304 CMR.

If we try to cut based on distance to reduce contamination by non-cluster members, we still find flatter slopes. If we define the center of the cluster as the location of the brightest elliptical (16:04:33.61, +43:21:04.0, J2000) and fit the E+S0 CMR within $0.5r_{200}$, we find a slope and intrinsic scatter of -0.034 ± 0.022 and 0.043 ± 0.010 . But this spatial cut excludes a spectroscopically confirmed elliptical galaxy ($z=0.9274$). Going out to $0.7r_{200}$ includes this galaxy, and we find a slope and intrinsic scatter of -0.019 ± 0.028 and 0.055 ± 0.015 (we exclude 1 S0 galaxy with $V_{606} - I_{814} = 1.59$). We list these different possible fits for the 4321 CMR to highlight the uncertainty of CMR fitting when the number of CMR galaxies is small, and spectroscopic membership is unknown. In this case the initial color and magnitude cuts have a large impact on the derived CMR.

3.4. Combined Cluster CMR

We can combine the galaxy samples because of the small redshift difference between the clusters. The difference in $V_{606} - I_{814}$ color between an early-type galaxy at $z = 0.90$ and $z = 0.92$ is small enough to be negligible (0.0008 AB mag for BC03 tau models). The fitting results are summarized in Table 3. The combined cluster CMR is shown in Figure 7, with the E+S0+Sa fit as the solid line, and the Coma relation as the dashed line. For the combined cluster E+S0 sample we find

$$(V_{606} - I_{814}) = (-0.068 \pm 0.010) \times (I_{814} - 23.) + 1.754 \pm 0.009$$

and an intrinsic scatter of 0.052 ± 0.006 mag. The combined CMR and this fit is shown in Figure 7. For the E-only sample, we find

$$(V_{606} - I_{814}) = (-0.070 \pm 0.013) \times (I_{814} - 23.) + 1.759 \pm 0.011$$

and an intrinsic scatter of 0.052 ± 0.007 mag. We find the same slopes, zeropoints, and scatters within the errors for all galaxy samples.

From the intrinsic scatter about the CMR for the E+S0 sample including 65 galaxies, we find an average age of $3.50_{-0.07}^{+0.13}$ Gyr, and $z_f = 2.4_{-0.06}^{+0.1}$ with the stochastic single burst model. The E-only sample of 42 galaxies has an intrinsic scatter of 0.052 ± 0.007 mag, identical to the E+S0 sample, so we also derive $t = 3.5$ Gyr and $z_f = 2.4$.

The combined cluster CMR has many spectroscopically confirmed cluster members, including 8 of the brightest 14 CMR galaxies. Fainter than $I_{814} \sim 22.2$ we note that the spectroscopic members tend to be bluer than the CMR, likely due to the combination of color and R -band selection. There are only three S0/a galaxies in the fit, and they are all fainter than $I_{814} = 23.5$. The CMR appears to be populated fairly evenly by E and S0 galaxies in magnitude; no significant segregation is seen. As for the individual clusters, the measured CMR slope, zeropoint, and scatter for the E-only and S0-only combined populations are consistent within the errors.

4. CLUSTER COMPARISON

In this section we compare the slopes, zeropoints, and scatters of the C11604+4304 and 4321 CMR relations. As stated in the previous section, we can directly compare the CMRs because of the small redshift difference between the clusters.

For the E+S0 sample, we find slopes consistent at the $\sim 1.4\sigma$ level (-0.076 ± 0.009 vs. -0.045 ± 0.021), with the formally steeper slope belonging to C11604+4304. As discussed in § 3.3, the 4321 CMR is less defined and more problematic to fit. A difference in CMR slopes is not ruled out, given the incompleteness of the spectroscopic samples. For the elliptical galaxies only, the slopes are in agreement: -0.074 ± 0.012 vs. -0.066 ± 0.027 , as are the S0-only slopes (-0.080 ± 0.016 vs. -0.045 ± 0.042).

The slope of the CMR can be used as a diagnostic of the average age of the galaxies (Kodama & Arimoto 1997; Gladders et al. 1998). Within 4 Gyr of formation, more metal-rich galaxies become redder faster than more metal-poor ones, and an initially flatter slope becomes steeper. Thus, if the CMR galaxies formed independently of mass (magnitude), within 4 Gyr of formation, the slope should be flatter than its $z = 0$ value, because the brighter galaxies are bluer with respect to their final colors than the less luminous galaxies.

To get an idea of the range of slopes one would expect at this redshift, in Figure 6 we show the C11604+4304 CMR with our fitted CMR relation as a solid line, the 4321 relation as a dash-dot line, and three models from Kodama & Arimoto (Kodama & Arimoto 1997) with formation redshifts of $z_f = 2, 3,$ and 5 . The model CMR relations are summarized in Table 4. The slopes become steeper as the formation redshift increases, mostly from the bright end of the CMR becoming redder. All three model slopes are too flat to match the faint end of the C11604+4304 CMR relation, but the $z_f = 2$ model matches the CMR relation of 4321. If the zeropoint of 4321 were not redder than C11604+4304, then we would interpret the marginally flatter slope as a consequence of a larger formation redshift for 4321. Basically, the slope for 4321 is flatter because the galaxies are redder at a given magnitude, which is inconsistent with younger

ages.

The zeropoints of the E+S0 and E-only relations are significantly different between Cl1604+4304 and 4321 ($2.1 - 2.6\sigma$). The Cl1604+4304 zeropoint is bluer in both cases, by about 0.04 magnitudes. This can be seen in Figure 6. This is caused by faint galaxies in Cl1604+4321 that are redder than the faint galaxies in Cl1604+4304 ($(V_{606} - I_{814}) = 1.7 - 1.9$ vs. $1.5 - 1.7$). If they are cluster members, this would imply they are either older or more metal-rich than galaxies of corresponding brightness in Cl1604+4304. Given Cl1604+4321's lower mass and lack of bright ellipticals, it would be surprising if the low-mass end of the CMR contains older or more metal-rich elliptical galaxies. We think it more likely that the low mass end of the Cl1604+4321 is not yet or only partially formed, and the faint, red, elliptical galaxies are interlopers, pushing the zeropoint redder, and the slope flatter. More extensive spectroscopy of the Cl1604 supercluster region indicates that there is a background structure at $z = 1.1 - 1.2$ in the Cl1604+4321 field (R. Gal, private communication).

The intrinsic scatters for all samples are not significantly different between the two clusters, implying similar ages and formation redshifts. This is the result we derive if we initially clip the 4321 sample around the Cl1604+4304 CMR. If we instead use a similar color cut and 2.4σ clipping, then 4321, the lower mass cluster, has a much larger scatter, corresponding to an average age difference of ~ 0.4 Gyr between Cl1604+4304 and 4321, for both the E+S0 and elliptical-only populations.

5. CMR SCATTER AS A FUNCTION OF MAGNITUDE

With all the evidence that less massive galaxies form their stars at later times than more massive galaxies, the 'downsizing' concept (Cowie et al. 1996), assuming a constant scatter about the CMR as a function of magnitude may not be correct. If the downsizing phenomenon also occurs for CMR galaxies, then not only should the average color become bluer with magnitude (decreasing mass), but the range in colors should also increase, increasing the measured scatter with magnitude. We investigate the dependence of the CMR on galaxy luminosity (mass) by first fitting the CMR in restricted magnitude ranges, then fixing the CMR slope and zeropoint from the fit to the bright end and calculating the intrinsic scatter about this relation.

There are too few galaxies in the Cl1604+4321 sample for meaningful measurements, so we focus on Cl1604+4304 and the combined sample. For Cl1604+4304, the intrinsic scatter about the CMR for galaxies with $20.5 \leq I_{814} < 22.5$ (bright end; $M_B \sim -22.5$ to -20.8) is 0.025 ± 0.005 magnitudes, and 0.039 ± 0.005 mag for the range $22.5 \leq I_{814} \leq 24$. (faint end; $M_B \sim -20.8$ to -19.5), a 2σ difference. The slope differences are suggestive, but not statistically significant: -0.052 ± 0.045 at the bright end, and -0.096 ± 0.020 at the faint end.

For the combined cluster sample, at the bright end, we find $(V_{606} - I_{814}) = (-0.040 \pm 0.024) \times (I_{814} - 23.) + 1.780 \pm 0.029$ and an intrinsic scatter of 0.030 ± 0.005 mag. There are no S0/a galaxies in the bright sample.

We also fit the faint end and restricted the initial sample to be between $1.5 \leq (V_{606} - I_{814}) \leq 1.95$. For the

E+S0 sample, we find a steeper slope of -0.089 ± 0.024 , a zeropoint of 1.759 ± 0.010 , and an intrinsic scatter of 0.045 ± 0.006 . The elliptical-only scatter also increases with magnitude, from 0.024 ± 0.004 mag to 0.043 ± 0.009 . These differences in scatter are significant at the $\sim 2\sigma$ level.

For the combined cluster population, we fix the slope at -0.068 and zeropoint at 1.754, as we found for the combined E+S0 population, and measure the scatter at the bright and faint end about this relation. For the E+S0 population, we find intrinsic scatters of 0.034 ± 0.005 mag at the bright end, and 0.048 ± 0.006 mag at the faint end, a 1.8σ result. For the elliptical-only population fixing the slope and zeropoint at -0.070 and 1.759, we find 0.030 ± 0.005 mag at the bright end, and 0.050 ± 0.007 mag at the faint end, a 2.3σ result.

Summarizing these results, with both methods, 1) an independent fitting of the slope, zeropoint, and scatter of the CMR at bright and faint ends, and 2) fixing the slope and the zeropoint from the full fit and compute the scatter about this relation for the bright and the faint ends, we detect marginally significant (2σ) increases in scatter with magnitude in the E+S0 and elliptical populations. The difference in scatter amounts to an age difference of ~ 0.15 Gyr with the solar metallicity single burst models.

Similar results have been previously reported. Tanaka et al. (2004) found increasing scatter about the CMR found in groups at $z = 0.83$, although they did not find evidence for this in their observed cluster, RXJ0152.7-1357, which we speculate is due to large photometric errors relative to ACS. A dependence of CMR scatter on CMR galaxy properties has been found in the studies of MS 1054-03 by van Dokkum et al. (2000) and Blakeslee et al. (2006). Restricting the sample to early-type galaxies brighter than $i_{775} < 22.5$ magnitude and excluding merger candidates, the rest-frame $U - B$ scatter is 0.024 ± 0.006 mag. But including merger candidates and all early-types down to $i_{775} = 23$ magnitudes, they found an intrinsic scatter of 0.052 ± 0.009 mag.

An increase of scatter and steepening of the slope compared to $z = 0$ would be expected if fainter galaxies are on average younger. If all CMR galaxies formed at the same time, but with metallicity varying with mass, there should be no increase in scatter, or possibly a decrease in scatter. An increase in scatter at faint magnitudes is expected if lower mass galaxies form their stars at later times, and the expected offset from the CMR of the higher mass galaxies should be bluewards.

6. DISCUSSION

Cl1604+4304 and 4321 are at the low-mass end of previously studied clusters at $z \sim 1$, so the comparison of the early-type CMR to other high redshift clusters should give us important information about the variation in formation times of cluster early-type galaxies. A significant uncertainty in comparing the CMR slopes between clusters is in the transformation from the observed slope to rest-frame $|\delta(U - B)/\delta B|$, as this is dependent on the spectral templates used for the transformation. For consistency with our comparison sample, we use the same templates used for the Cl1604 slope and scatter transformation (see §3) to transform the observed CMR slopes for the elliptical-only samples for MS 1054 and Cl 0152-1357 (Blakeslee et al. 2006), Cl0910+5442 (Mei et al.

2006a), C11252-2927 (Blakeslee et al. 2003b), and Lynx E+W (Mei et al. 2006b). We list the slopes and the transformations in Table 5. We note that the quoted slope measurements are made over different absolute magnitude ranges, which may lead to different derived CMR slopes. Another complication is in the filter transformations, i.e. how well is the underlying galaxy spectral energy distribution matched by the templates used to derive these transformations.

The three clusters at $z \sim 0.9$, MS 1054-03, RX J0152.7-1357, and C11604, span a large range of slopes, and it is unclear if this is significant. The MS 1054 and RX J0152.7-1357 slopes were fitted with a magnitude limit about 1 magnitude fainter than C11604, and were fitted using *only* spectroscopically confirmed cluster members. If we fit the C11604 elliptical-only sample at the same limiting magnitude, we find a much shallower CMR slope ($|\delta(U - B)/\delta B| = 0.027 \pm 0.014$) that is in agreement with both RX J0152.7-1357 and MS 1054-03. For C11604, the fitted CMR slope at the bright end is consistent with other clusters at intermediate redshift (van Dokkum et al. 2000; Blakeslee et al. 2003b; Mei et al. 2006a,b; Blakeslee et al. 2006), but the galaxies at the faint end are relatively bluer, pushing the composite slope steeper. The only cluster with a comparably steep slope is Lynx W, however, only 6 galaxies contribute to this slope. Trends of CMR slope with cluster mass and X-ray properties will be discussed in Mei et al. (2006c).

The average formation redshifts of early-type galaxies derived here, $z_f = 2.4 - 2.6$, agree well with those from previous cluster studies: $z_f \approx 2.2$ at $z = 0.83$ (Blakeslee et al. 2006), $z_f \approx 2.3$ at $z = 1.10$ (Mei et al. 2006a), and $z_f \approx 2.8$ at $z = 1.27$ (Mei et al. 2006b). We measured the scatter about the CMR in restricted magnitude ranges, and find that scatter increases as a function of magnitude.

Wake et al. (2005) studied 12 clusters at $z \sim 0.3$ covering a factor of 100 in X-ray luminosity, and put an upper limit of 2 Gyr on the average variation in CMR galaxy ages from the lack of observed dependence of CMR zeropoint on X-ray luminosity. Our results are not inconsistent with this, as an age range of 2 Gyr is quite large, much larger than the range of < 1 Gyr that we probe here. They also noted that the 5 least X-ray luminous clusters ($0.1 - 0.7 \times 10^{44} \text{ erg s}^{-1}$) had sparse CMRs, forcing them to combine clusters to measure a composite faint X-ray cluster CMR. We find a similar qualitative difference in the color-magnitude diagrams and CMRs of C11604+4304 and 4321. There is a lack of bright, $M_B < -20.9$ elliptical galaxies in 4321, possibly because mass assembly/BCG formation in 4321 is incomplete.

The CMR scatters and slopes of the $z = 1.27$ Lynx E and W clusters were found to depend on distance from the cluster center (Mei et al. 2006b), increasing and steepening as the distance increased. We find no such dependence for either cluster sample, but the number of galaxies is small and the radial coverage is slightly less than 1 Mpc. We also find no difference in the CMR relations for the E and S0 galaxies separately. So far, only one study has found a difference in the E and S0 cluster populations at $z \sim 1$. (Mei et al. 2006a) found that the CMR for S0s in C10910 ($z = 1.10$,

$L_{X,Bol} = 2.5_{-0.3}^{+0.3} \times 10^{44} \text{ erg s}^{-1}$; Stanford et al. 2002b) had a significantly bluer zeropoint than for the ellipticals, implying younger ages or lower metallicities at similar luminosity.

The intrinsic scatter for the combined cluster sample agrees well with other clusters at similar redshifts, confirming a lack of measured evolution of scatter about the CMR down to low cluster X-ray luminosities. This lack of evolution in the measured scatter could be due to a combination of 'progenitor bias' (van Dokkum & Franx 2001) and the fitting technique. We found that the intrinsic scatter increases as a function of magnitude, and is significantly larger for CMR galaxies from $0.15 - 0.4L^*$ in our combined cluster sample. The combination of galaxies within $0.5 - 2L^*$ having similar properties over a range of environment, and fewer CMR galaxies with $L < 0.4L^*$ present at $z \sim 1$ (e.g. De Lucia et al. 2004) could 'conspire' to keep the measured scatters constant. As also discussed in Holden et al. (2004), by sigma-clipping around the CMR, we are selecting the oldest cluster galaxies at any given redshift, not the cluster population that will evolve into the $z = 0$ CMR population.

Although the CMR is observed in large area galaxy surveys out to $z = 1$ (Bell et al. 2004; McIntosh et al. 2005), we know that the CMR evolves. Striking evidence for the formation of the CMR and its dependence on environment was recently demonstrated by Tanaka et al. (2004). While there is a clear CMR in the field, groups, and clusters at $z = 0$, the field CMR is not present at $z = 0.83$, and becomes less defined in groups at $z = 0.83$ and $m > M^* + 2$. This was detected as an increase in CMR scatter as a function of increasing magnitude. Building on this theme, we find no evidence for evolution, other than passive, in the bright end of the CMR ($L \gtrsim 0.5L^*$), in agreement with many other studies (van Dokkum et al. 2000; Blakeslee et al. 2003b; Holden et al. 2004; Mei et al. 2006a,b; Blakeslee et al. 2006). However, considering CMR galaxies down to $0.15L^*$, we find tentative evidence for a dependence of CMR slope on cluster X-ray luminosity or mass, in the sense that less luminous clusters have steeper slopes. If this is confirmed by further studies, it must be due to a combination of 'downsizing', where the fainter, less massive CMR galaxies form later than the brighter, more massive ones in a given cluster, and an overall younger age for faint CMR galaxies in the lower mass clusters. If 'downsizing' were not invoked, meaning all CMR galaxies form simultaneously, then younger clusters should have flatter slopes.

Earlier studies of the scatter in lower redshift clusters could only put a lower limit of $z_f > 1 - 1.5$ for the average formation redshift of the CMR galaxies (e.g. van Dokkum et al. 1998). Now that we can observe galaxy clusters in this redshift range, we can put much stronger constraints on their formation redshifts. The range $z = 3 - 5$ is emerging as crucial for understanding the formation of massive cluster ellipticals and their transition from rapidly star-forming to passive. Although semianalytic and hydrodynamic models of galaxy formation are now able to reproduce a color bimodality of galaxies from $z = 0 - 1$ (Dave et al. 2005; Kang et al. 2005; Menci et al. 2005), they still produce bright blue galaxies at $z = 0$, the SFRs of most model red galaxies decline only slowly after $z = 2$, and is driven by major

merging events (Menci et al. 2005). The star formation decline is much too slow to reproduce the tight CMRs found in $z \sim 1$ clusters, and major merging including gas (dissipative mergers) is not observed to occur for a significant fraction of massive cluster galaxies. What these models probably do get right is that the color bimodality of galaxies is driven by major differences in their progenitor star formation histories at $z = 4 - 5$, which we can hopefully test by continuing to push our observations outward in redshift.

7. CONCLUSIONS

We presented an analysis of the color-magnitude relation in Cl1604+4304 ($z = 0.90$) and Cl1604+4321 ($z = 0.92$), both part of the 16h supercluster (Gal & Lubin 2004). Based on their X-ray luminosities, both of these clusters are at the low mass end of the range of previously studied clusters at $z = 0.8 - 1.3$. Our main conclusions are as follows.

- Both Cl1604+4304 and 4321 have identifiable early-type color-magnitude relations. However, Cl1604+4321, the less massive of the two clusters, lacks bright M^* ellipticals, and we suggest that it has not yet had time to assemble bright early-type red sequence members. From our analysis of the CMR relations, we find a redder zeropoint for 4321. The CMR slope and scatter depend strongly on our choice of initial color cuts, and the possibility of significant differences in slope and scatter between Cl1604+4304 and 4321 is open.
- The slope of the combined cluster CMR is significantly steeper than for RX J0152.7-1357 but con-

sistent with MS 1054-03, both at similar redshift. This may be due to the difference in magnitude limit used for the fitting, the different observed filters, or a real difference in the galaxy populations. The slope of the CMR at the bright end ($0.5 - 2 L^*$) is flatter and consistent with the CMR slopes found for other high redshift clusters.

- From the intrinsic scatter about the CMR for the full sample of 65 E+S0 galaxies, we find an average galaxy age of $3.50^{+0.13}_{-0.07}$ Gyr, and an average $z_f = 2.4^{+0.1}_{-0.06}$.
- We find evidence for an increasing intrinsic scatter with increasing magnitude, previously only known in the group and field environment at these redshifts. This implies an decreasing mean galaxy age with decreasing galaxy mass, of about 0.15 Gyr from $\sim 1L^*$ to $\sim 0.3L^*$.

ACS was developed under NASA contract NAS 5-32865, and this research has been supported by NASA grant NAG5-7697 and by an equipment grant from Sun Microsystems, Inc. The Space Telescope Science Institute is operated by AURA Inc., under NASA contract NAS5-26555. We are grateful to K. Anderson, J. McCann, S. Busching, A. Framarini, S. Barkhouser, and T. Allen for their invaluable contributions to the ACS project at JHU. We thank W. J. McCann for the use of the FITSCUT routine for our color images.

REFERENCES

- Beers, T. C., Flynn, K., & Gebhardt, K. 1990, *AJ*, 100, 32
 Bell, E. F., et al. 2004, *ApJ*, 608, 752
 Benítez, N., et al. 2004, *ApJS*, 150, 1
 Bertin, E., & Arnouts, S. 1996, *A&AS*, 117, 393
 Bernardi, M., Sheth, R. K., Nichol, R. C., Schneider, D. P., & Brinkmann, J. 2005, *AJ*, 129, 61
 Blakeslee, J. P., Anderson, K. R., Meurer, G. R., Benítez, N., & Magee, D. 2003a, *Astronomical Society of the Pacific Conference Series*, 295, 257
 Blakeslee, J. P., et al. 2003b, *ApJ*, 596, L143
 Blakeslee, J. P., et al. 2006, *ApJ*, submitted
 Bower, R. G., Lucey, J. R., & Ellis, R. S. 1992, *MNRAS*, 254, 601
 Bruzual, G., & Charlot, S. 2003, *MNRAS*, 344, 1000
 Castander, F. J., Ellis, R. S., Frenk, C. S., Dressler, A., & Gunn, J. E. 1994, *ApJ*, 424, L79
 Coleman, G. D., Wu, C.-C., & Weedman, D. W. 1980, *ApJS*, 43, 393
 Cowie, L. L., Songaila, A., Hu, E. M., & Cohen, J. G. 1996, *AJ*, 112, 839
 Dave, R., Finlator, K., Hernquist, L., Katz, N., Keres, D., Papovich, C., Weinberg, D. 2005, "The Faculous Destiny of Galaxies: Bridging Past and Present", Marseille, France, astro-ph/0510625
 de Vaucouleurs, G., de Vaucouleurs, A., Corwin, H. G., Buta, R. J., Paturel, G., & Fouque, P. 1991, Volume 1-3, XII, 2069 pp. 7 figs.. Springer-Verlag Berlin Heidelberg New York
 De Lucia, G., et al. 2004, *ApJ*, 610, L77
 Ford, H. C., et al. 2003, *Proc. SPIE*, 4854, 81
 Gal, R. R., & Lubin, L. M. 2004, *ApJ*, 607, L1
 Gladders, M. D., Lopez-Cruz, O., Yee, H. K. C., & Kodama, T. 1998, *ApJ*, 501, 571
 Gladders, M. D., & Yee, H. K. C. 2005, *ApJS*, 157, 1
 Gunn, J. E., Hoessel, J. G., & Oke, J. B. 1986, *ApJ*, 306, 30
 Högbom, J. A. 1974, *A&AS*, 15, 417
 Hogg, D. W., et al. 2004, *ApJ*, 601, L29
 Holden, B. P., Stanford, S. A., Eisenhardt, P., & Dickinson, M. 2004, *AJ*, 127, 2484
 Holden, B. P., et al. 2005, *ApJ*, 626, 809
 Kang, X., Jing, Y. P., Mo, H. J., Boumlrner, G. 2005, *ApJ*, 631, 21
 Kinney, A. L., Calzetti, D., Bohlin, R. C., McQuade, K., Storchi-Bergmann, T., & Schmitt, H. R. 1996, *ApJ*, 467, 38
 Kodama, T., & Arimoto, N. 1997, *A&A*, 320, 41
 Lubin, L. M., Postman, M., Oke, J. B., Ratnatunga, K. U., Gunn, J. E., Hoessel, J. G., & Schneider, D. P. 1998, *AJ*, 116, 584
 Lubin, L. M., Brunner, R., Metzger, M. R., Postman, M., & Oke, J. B. 2000, *ApJ*, 531, L5
 Lubin, L. M., Mulchaey, J. S., & Postman, M. 2004, *ApJ*, 601, L9
 McIntosh, D. H., Zabludoff, A. I., Rix, H.-W., & Caldwell, N. 2005, *ApJ*, 619, 193
 Mei, S. et al. 2006a, *ApJ*, 639, 81
 Mei, S. et al. 2006b, *ApJ*, in press
 Menci, N., Fontana, A., Giallongo, E., & Salimbeni, S. 2005, *ApJ*, 632, 49
 Nelan, J. E., Smith, R. J., Hudson, M. J., Wegner, G. A., Lucey, J. R., Moore, S. A. W., Quinney, S. J., & Suntzeff, N. B. 2005, *ApJ*, 632, 137
 Norberg, P., et al. 2002, *MNRAS*, 336, 907
 Oke, J. B., Postman, M., & Lubin, L. M. 1998, *AJ*, 116, 549
 Press, W. H., Teukolsky, S. A., Vetterling, W. T., & Flannery, B. P. 1992, Cambridge: University Press, —c1992, 2nd ed.,
 Peng, C. Y., Ho, L. C., Impey, C. D., & Rix, H. 2002, *AJ*, 124, 266
 Postman, M., Lubin, L. M., & Oke, J. B. 1998, *AJ*, 116, 560
 Postman, M., Lubin, L. M., & Oke, J. B. 2001, *AJ*, 122, 1125
 Postman, M. et al., *ApJ*, 623, 721
 Sirianni, M., et al. 2005, *PASP*, 117, 1049
 Stanford, S. A., Eisenhardt, P. R., & Dickinson, M. 1998, *ApJ*, 492, 461

- Stanford, S. A., Eisenhardt, P. R., Dickinson, M., Holden, B. P., & De Propris, R. 2002, *ApJS*, 142, 153
- Stanford, S. A., Holden, B., Rosati, P., Eisenhardt, P. R., Stern, D., Squires, G., & Spinrad, H. 2002, *AJ*, 123, 619
- Tanaka, M., Goto, T., Okamura, S., Shimasaku, K., & Brinkmann, J. 2004, *AJ*, 128, 2677
- van Dokkum, P. G., Franx, M., Fabricant, D., Illingworth, G. D., & Kelson, D. D. 2000, *ApJ*, 541, 95
- van Dokkum, P. G., & Franx, M. 2001, *ApJ*, 553, 90
- van Dokkum, P. G., & Stanford, S. A. 2003, *ApJ*, 585, 78
- Visvanathan, N., & Sandage, A. 1977, *ApJ*, 216, 214
- Wake, D. A., Collins, C. A., Nichol, R. C., Jones, L. R., Burke, D. J. 2005, *ApJ*, in press, astro-ph/0503480

TABLE 1
CL1604+4304

Sample	N_{gal}	Zeropoint	Slope	σ_{int}	$\delta(U - B)_z/\delta B$	$\sigma_{int}(U - B)_z$
E+S0	38	1.738±0.008	-0.076±0.009	0.038±0.004	-0.061±0.007	0.030±0.003
E	23	1.739±0.011	-0.074±0.012	0.038±0.006	-0.059±0.009	0.030±0.004
S0	15	1.738±0.012	-0.080±0.016	0.033±0.007	-0.064±0.012	0.026±0.005

NOTE. — For galaxies brighter than $I_{814} = 24$ mag. Errors on the rest-frame U-B slopes and scatters do not include errors from the transformation.

TABLE 2
CL1604+4321

Sample	N_{gal}	Zeropoint	Slope	σ_{int}	$\delta(U - B)_z/\delta B$	$\sigma_{int}(U - B)_z$
E+S0+Sa	30	1.769±0.015	-0.053±0.021	0.059±0.008	-0.042±0.015	0.043±0.006
E+S0	27	1.782±0.015	-0.045±0.021	0.053±0.010	-0.036±0.015	0.040±0.007
E	19	1.783±0.018	-0.066±0.027	0.048±0.011	-0.053±0.020	0.036±0.009
S0	9	1.47±0.63	-0.045±0.042	0.052±0.024	-0.036±0.031	0.039±0.018

NOTE. — For galaxies brighter than $I_{814} = 24$ mag. Errors on the rest-frame U-B slopes and scatters do not include errors from the transformation.

TABLE 3
COMBINED CLUSTER SAMPLE

Sample	N_{gal}	Zeropoint	Slope	σ_{int}	$\delta(U - B)_z/\delta B$	$\sigma_{int}(U - B)_z$
E+S0+Sa	69	1.753±0.009	-0.065±0.011	0.055±0.006	-0.052±0.008	0.044±0.005
E+S0	65	1.754±0.009	-0.068±0.010	0.052±0.006	-0.054±0.008	0.042±0.005
E	42	1.759±0.011	-0.070±0.013	0.052±0.007	-0.056±0.010	0.042±0.006
S0	22	1.740±0.010	-0.070±0.013	0.041±0.006	-0.056±0.010	0.033±0.005

NOTE. — For galaxies brighter than $I_{814} = 24$ mag. For the S0 fit we used an initial color cut of $1.55 \leq V_{606} - I_{814} \leq 1.95$.

TABLE 4
KODAMA-ARIMOTO MODELS

z formation	CMR Slope	CMR Zeropoint
2	-0.036	1.78
3	-0.047	1.81
5	-0.047	1.84

TABLE 5
REST-FRAME CMR ELLIPTICAL-ONLY SLOPES

Cluster	Redshift	Observed Slope	transformation	$-\delta(U - B)/\delta B$	Reference
Coma		-0.079 ± 0.007	$slope(U - B) = 0.66 slope(U - V)$	0.052 ± 0.005	(1)
RX J0152.7-1357	0.83	-0.007 ± 0.011	$slope(U - B) = 1.19 slope(r_{625} - i_{775})$	0.008 ± 0.013	(2)
MS 1054-03	0.83	-0.042 ± 0.014	$slope(U - B) = 0.91 slope(V_{606} - i_{775})$	0.038 ± 0.013	(2)
Cl 1604	0.91	-0.070 ± 0.013	$slope(U - B) = 0.79 slope(V_{606} - I_{814})$	0.055 ± 0.010	
Cl 0910	1.10	-0.033 ± 0.015	$slope(U - B) = 1.12 slope(i_{775} - z_{850})$	0.037 ± 0.017	(3)
Cl 1252-2927	1.24	-0.020 ± 0.009	$slope(U - B) = 1.72 slope(i_{775} - z_{850})$	0.034 ± 0.015	(4)
Lynx E	1.27	-0.025 ± 0.012	$slope(U - B) = 1.79 slope(i_{775} - z_{850})$	0.045 ± 0.021	(5)
Lynx W	1.27	-0.043 ± 0.015	$slope(U - B) = 1.79 slope(i_{775} - z_{850})$	0.077 ± 0.027	(5)

NOTE. — (1) Bower et al. (1992), (2) Blakeslee et al. (2006), (3) Mei et al. (2006a), (4) Blakeslee et al. (2003b), (5) Mei et al. (2006b)

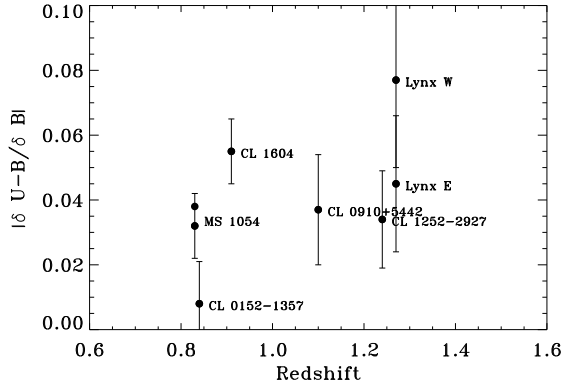


FIG. 1.— Rest-frame $|\delta(U - B)/\delta B|$ CMR slopes vs. cluster redshift.

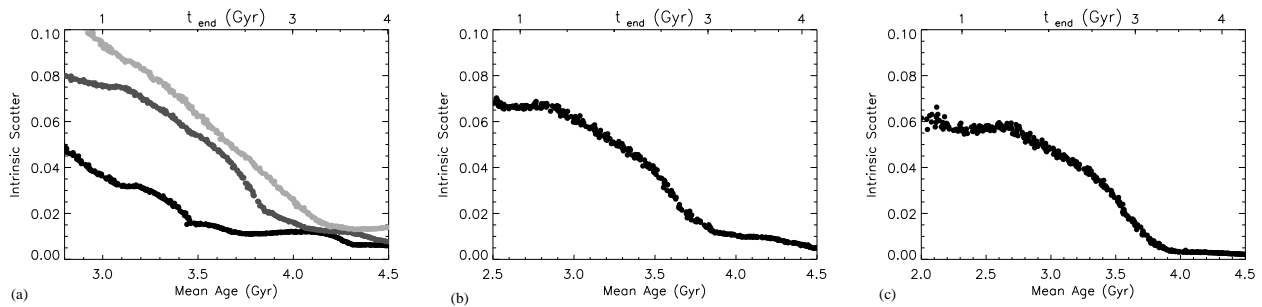


FIG. 2.— Intrinsic scatter in $V_{606} - I_{814}$ at $z = 0.9$ vs. luminosity-weighted mean galaxy age and t_{end} with different models. From left to right: (a) single bursts with $Z=0.008$ (black), $Z=0.02$ (medium gray), $Z=0.05$ (light gray), (b) exponentially declining star formation rates with $\tau = 1$ and solar metallicity, (c) constant star formation rates between t_1 and t_2 chosen at random between t_0 and t_{end} . In all three models, the minimum t_{end} is 0.5 Gyr ($z=1.02$).

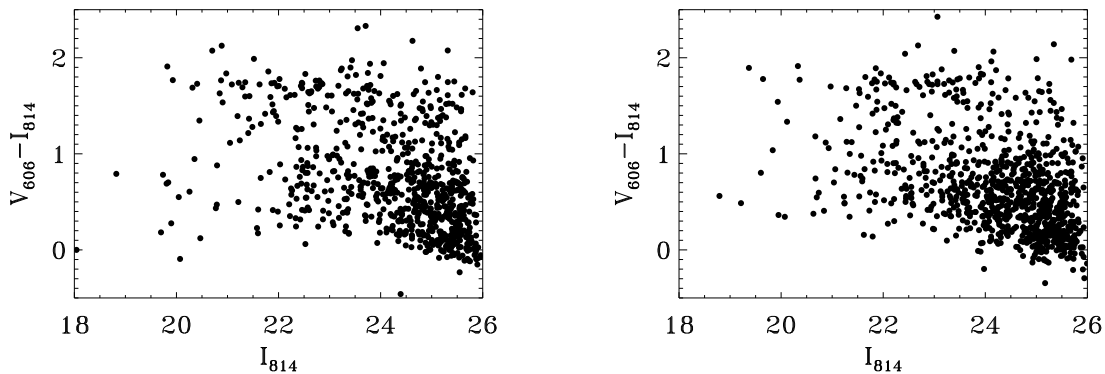


FIG. 3.— Color magnitude diagrams of the cluster fields: Cl1604+4304 (left) and Cl1604+4321 (right).

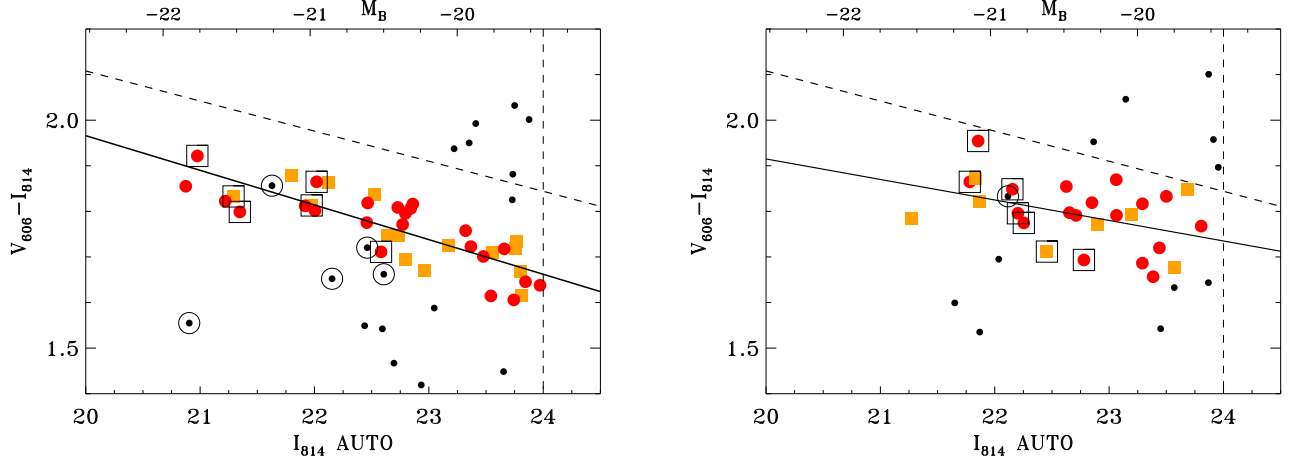


FIG. 4.— CL1604+4304 (left) and CL1604+4321 (right) color magnitude relations. Visual morphological types are indicated by circles (Es) and squares (S0s). Red sequence members are indicated by red circles (Es) and orange squares (S0s). Open boxes indicate spectroscopically confirmed cluster members. Open circles indicate spectroscopically confirmed interlopers. The small dots are early-type galaxies that are not included in the fit. These include the galaxies rejected by the iterative fit and the spectroscopically confirmed interlopers. The CMR fit to the E+S0 sample is overplotted as a solid line. We do not plot the other (E, S0, E+S0+Sa) relations because they are so similar to this relation. The black dashed line is the transformed Coma relation.

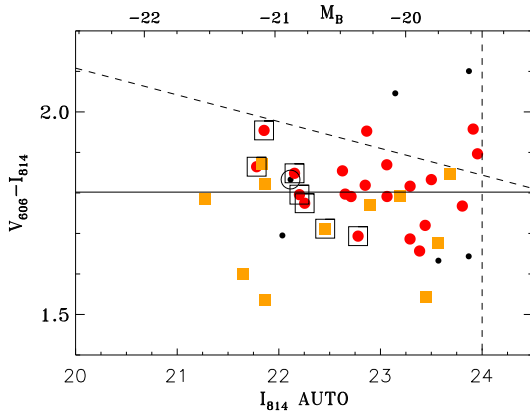


FIG. 5.— CL1604+4321 CMR using the same color cuts and sigma clipping as for CL1604+4304, instead of an initial cut around the CL1604+4304 CMR. Symbols are the same as for Fig. 4. The solid line is the fit to the E+S0 sample.

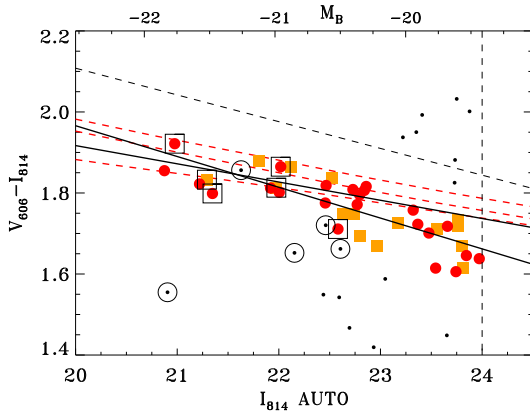


FIG. 6.— CL1604+4304 with three CMR models from Kodama & Arimoto with formation redshifts of 2, 3, and 5 (dashed lines, from bluer to redder). Galaxy symbols are the same as in Figure 4. The solid lines are the CL1604+4304 and 4321 E+S0 CMRs (+4304 is steeper). The black dashed line is the transformed Coma relation.

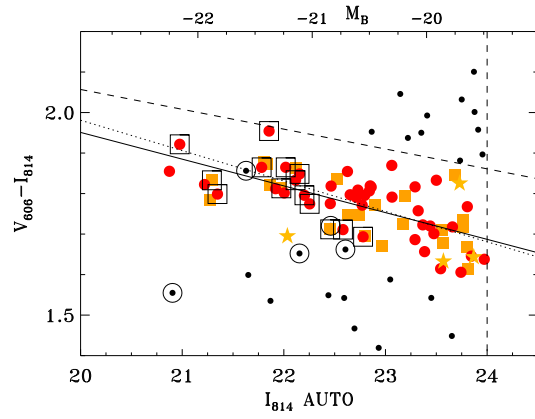


FIG. 7.— The combined cluster sample. Galaxy symbols are the same as in Figure 4, including S0/a galaxies as orange stars. The CMR fit to the full sample is overlotted as the solid line. This fit to only the Es is the dotted line. The dashed line is the transformed Coma relation.